



Modified predictive torque control method of induction machines for torque ripple reduction

Dubravko Krušelj^a and Damir Sumina^b

^aKončar – Electronics and Informatics, Inc., Zagreb, Croatia; ^bUniversity of Zagreb Faculty of Electrical Engineering and Computing, Zagreb, Croatia

ABSTRACT

Direct torque control, model predictive control and field oriented control are control methods mostly used in high performance induction machine drives. In the direct torque control method, control variables are estimated from the stator variables, and the only parameter required is the stator resistance. The predictive torque control with horizon one has recently attracted much research attention but it requires the use of the induction machine speed, and both the stator and the rotor parameters, usually requires adjustment of the weighting factors, and has high computational burden. This paper proposes a modified predictive torque control method of induction machines. The estimated and predicted values are calculated from the stator variables, and the method uses the cost function without the weighting factor. When the two-level three-phase voltage source inverter is analyzed, it is shown that the predicted values should be calculated for three voltage vectors. The modified predictive torque control results in a better steady state performance regarding torque ripple in comparison with the conventional direct torque control and the predictive torque control methods. Simulation and experimental results for the main propulsion drive of the low-floor tram are presented in order to validate the effectiveness of the proposed method.

ARTICLE HISTORY

Received 15 November 2018
Accepted 29 April 2019

KEYWORDS

Induction machine; traction; direct torque control; model predictive control; predictive torque control; torque ripple; stator flux ripple

1. Introduction

Field oriented control (FOC) and direct torque control (DTC) have been two control methods mostly used for induction machine (IM) drives that require high performances [1,2]. The basics of the DTC method were introduced in the mid 1980s by M. Depenbrock as direct self-control [3,4] and by I. Takahashi as conventional DTC method [5]. A commercialization of the DTC method began in the mid 1990s [6] and since then the method has been further analyzed and improved. The features of the DTC method are described in [1,7] and the DTC method is compared with the FOC regarding steady state and transient performances, parameter sensitivity and implementation complexity in [2,8].

The main advantage of the DTC method in comparison with the FOC is its simplicity and robustness. The only required IM parameter is the stator resistance, the control variables (the electromagnetic torque and the stator flux vector) are calculated from the stator variables, and are directly controlled, and coordinate transformation, current controllers and a PWM signal generator are not required. Although the DTC method structure is simple, a very quick dynamic response of the control variables can be achieved. Nevertheless, the DTC method suffers from its disadvantages: relatively

high torque, high current ripple, variable switching frequency, lack of direct current control and difficulty to control the torque and stator flux at a very low speed. For the application of the DTC method in e.g. traction drives, the stable operation in the low speed range should be achieved and it is also desirable to decrease the torque ripple.

The method introduced in [5] is considered as the conventional method for DTC of IMs and many different modified methods for DTC have been developed in order to either cancel or diminish the influence of the above mentioned disadvantages. The modified DTC methods can be categorized in several groups with some common features [9]: methods with variable duty cycle, methods with space vector modulation (SVM), modified methods for the operation in the low speed range and model predictive control (MPC) methods. The advances in the DTC method and various adopted strategies are also presented in [10] and a review of the DTC method with improvements can be found in [11].

The MPC methods have recently received significant attention in the field of power electronics [12–16]. The MPC methods can be applied in converters with multiple switches and nonlinearities and constraints can be easily included. The MPC is also referred to as receding horizon control and the key element underlying the

MPC is that of the moving horizon optimization. The special case of the MPC is when the horizon length is set to one and then the calculation of the optimal switching state is relatively simple and a controller can easily be implemented. The finite control set model predictive control (FCS-MPC) does not require a modulator and takes the discrete nature of the power converter into account. Since power converters have a finite number of switches, the optimization problem is reduced to the prediction of the system behaviour for possible switching states and the selection of the switching state, which minimizes the given cost function. The FCS-MPC with a horizon one and especially the predictive torque control (PTC) method have attracted the most research attention and are considered to be a powerful alternative to the FOC and the DTC in high performance IM drives [17–20]. The DTC and the FCS-MPC are nonlinear control methods in which voltage vectors are directly generated. Neither of the methods uses internal current control loops and SVM algorithm, which results in a very fast dynamic response. In both methods, the estimated and predicted values of the currents and fluxes are in the stator reference frame and no coordinate transformation is needed. There are yet some crucial differences between these methods. In the FCS-MPC method, for the prediction of the variables used in the cost function both the IM stator and rotor variables and parameters as well as the IM speed are used, which makes the method parameter dependent. On the other hand, the DTC method requires only the stator resistance and is inherently a sensorless method. The MPC method can handle several control objectives simultaneously and the variables that are controlled should be included in the cost function. The weighting factors used in the cost function have a direct influence on the performance of the system but their tuning is nontrivial work and there is no analytical or numerical solution to obtain an optimal solution, which even might restrict the application of the MPC method in practice. Another important drawback of the FCS-MPC method is its high computational burden due to the fact that the cost function should be calculated for all possible switching states. Many researchers have improved the MPC with a combination of modern control methods in order to make the MPC more reliable [21–27]. Some guidelines based on the empirical procedure for obtaining suitable weighting factors are given in [15,16,28], and there are methods which do not require weighting factors [23,29,30] or an optimized weighting factor can be determined online [25].

This paper proposes a modified predictive torque control (MPTC) method to be used for IMs. Control variables of the method are the electromagnetic torque and the stator flux vector magnitude which are estimated from the stator variables, and the stator resistance is the only required IM parameter. The MPTC method calculates predicted values of the

control variables from the stator variables and uses the cost function, which consists of the difference between the reference and the predictive value of the electromagnetic torque. In such a way, the use of the weighting factor is avoided. The MPTC method is based on the influence of the stator voltage vectors on the stator flux vector magnitude and the electromagnetic torque changes, which depend on the exact position of the stator flux vector in the complex plane. When a two-level three-phase voltage source inverter (VSI) is applied, predicted values should be calculated for three voltage vectors, which considerably reduces the computational burden. The MPTC method, the conventional DTC method and the PTC method with horizon one are compared regarding torque ripple, flux ripple and stator current total harmonic distortion (THD). Simulation and experimental results for the main propulsion drive of the low-floor tram series TMK 2200 operating in the city of Zagreb are presented in order to show the effectiveness of the method. It is shown that the proposed MPTC method shows better steady state performances regarding torque ripple in comparison with the conventional DTC and similar steady state performances as the PTC method with smaller values of the weighting factor.

2. MPTC method for IM drives

2.1. IM model

The IM equations used in the MPTC method are given in the stator reference frame:

$$\vec{u}_S = R_S \vec{i}_S + \frac{d\vec{\psi}_S}{dt} \quad (1)$$

$$\vec{\psi}_S = L_S \vec{i}_S + L_m \vec{i}_R \quad (2)$$

$$\vec{\psi}_R = L_m \vec{i}_S + L_R \vec{i}_R \quad (3)$$

$$t_{\text{elm}} = \frac{3}{2} p \text{Im}\{\vec{\psi}_S^* \cdot \vec{i}_S\} \quad (4)$$

where \vec{u}_S is the stator voltage vector, \vec{i}_S is the stator current vector, $\vec{\psi}_S$ is the stator flux vector, \vec{i}_R is the rotor current vector, $\vec{\psi}_R$ is the rotor flux vector, t_{elm} is the electromagnetic torque and R_S , L_S , L_m , L_R and p are the IM stator resistance, stator inductance, mutual inductance, rotor inductance and number of pole pairs, respectively.

The control variables of the MPTC method are the electromagnetic torque and the stator flux vector and are directly controlled with an adequate voltage vector. A two-level three-phase VSI can provide eight different voltage vectors in total, six active vectors and two zero voltage vectors. One voltage vector is applied during the whole control period, i.e. in the time period in which control signals are determined for inverter semiconductors. Figure 1 presents the voltage vectors in the complex plane, which is divided into six sectors and

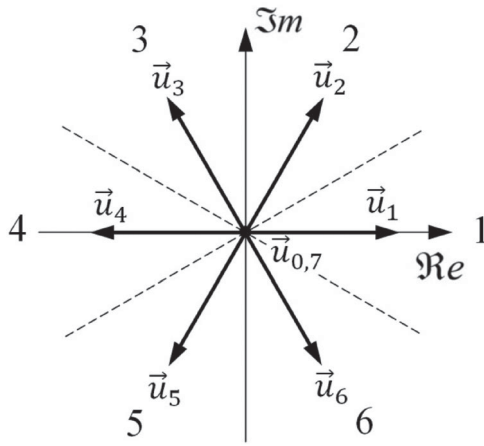


Figure 1. Voltage vectors and sectors in the complex plane.

each active stator voltage vector lies in the middle of the sector.

2.2. Prediction of the control variables at the beginning of a next control period

The stator flux vector is estimated by integrating the induction machine back electromotive force, Equation (1):

$$\vec{\psi}_S = \int \vec{u}_S dt - \int R_S \vec{i}_S dt \quad (5)$$

The first term on the right side of Equation (5) is calculated by integrating the stator voltage vector \vec{u}_S which is calculated from the control signals for inverter semiconductors, the measured value of the d.c. link voltage, the semiconductor voltage drops and the inverter dead time. The second term on the right side of Equation (5) is mostly defined by the time dependence of the stator current vector \vec{i}_S in the control period, because it might be assumed that the value of the stator resistance R_S does not change during a relatively short control period (typically few tens of μs). It can also be assumed that the stator currents changes are approximately linear during the control period [30]. The stator currents are usually measured at the beginning of the control period. In order to predict the stator current vector at the beginning of a next control period, e.g. a simple current prediction algorithm proposed in [31] can be used when the stator currents are measured once again within the control period. The stator current prediction can be further improved if one additional measurement is performed in the control period. The stator currents can be measured at the beginning of the control period, at the time instant which is greater than the time period when the turn on or turn off process is over, and then once again. The predicted value of the stator current vector at the beginning of a next, $(k+1)^{st}$ control period can be calculated using the following linear

extrapolation:

$$\vec{i}_S^P(k+1) = \frac{\vec{i}_{S2} - \vec{i}_{S1}}{t_2 - t_1}(\Delta T - t_1) + \vec{i}_{S1} \quad (6)$$

where $\vec{i}_S^P(k+1)$ is the predicted value of the stator current vector at the beginning of a next control period, ΔT is the control period and \vec{i}_{S1} , \vec{i}_{S2} are the stator current vectors calculated from measurements at time instants $t_1, t_2 (t_2 > t_1)$.

The stator flux vector at the beginning of a next control period can be predicted from Equation (5) by using an average value of the stator current vector in the control period:

$$\vec{\psi}_S^P(k+1) = \vec{\psi}_S(k) + \vec{u}_S(k)\Delta T - R_S \vec{i}_{SAV}(k)\Delta T \quad (7)$$

where $\vec{\psi}_S^P(k+1)$ is the predicted value of the stator flux vector at the beginning of a next control period and $\vec{i}_{SAV}(k)$ is an average value of the stator current vector in the control period.

The predicted electromagnetic torque at the beginning of the next control period is calculated from Equations (4, 6–7):

$$T_{elm}^P(k+1) = \frac{3}{2} p \text{Im}\{\vec{\psi}_S^P(k+1)^* \cdot \vec{i}_S^P(k+1)\} \quad (8)$$

where $T_{elm}^P(k+1)$ is the predicted electromagnetic torque at the beginning of a next control period.

In the real implementation, the calculation of the voltage vector which will be applied in a next control period takes almost the whole control period. The time delay due to the necessary calculations could be taken into account by a two-step prediction, i.e. the predicted values of the control variables at the beginning of the $(k+2)^{nd}$ control period should be calculated [17,18].

2.3. Influence of the voltage vectors on the stator flux vector and the electromagnetic torque

In a two-level three-phase VSI one of eight possible voltage vectors is applied for the whole control period ΔT and there is a change in the stator flux vector magnitude:

$$\Delta|\vec{\psi}_S| = |\vec{\psi}_S(t_k + \Delta T)| - |\vec{\psi}_S(t_k)| \quad (9)$$

where $\Delta|\vec{\psi}_S|$ is a change in the stator flux vector magnitude in the control period, $|\vec{\psi}_S(t_k + \Delta T)|$ is the stator flux vector magnitude at the end of the control period (value at time instant $t = t_k + \Delta T$) and $|\vec{\psi}_S(t_k)|$ is the stator flux vector magnitude at the beginning of the control period (value at time instant $t = t_k$).

Figure 2 shows a change of the stator flux vector in a general sector N where the stator voltage vector \vec{u}_N is aligned with the real axis. $\Delta\vec{\psi}_S$ is the vector which represents the change of the stator flux vector in the control period, $\varphi_S(t_k)$ is the stator flux vector angle at

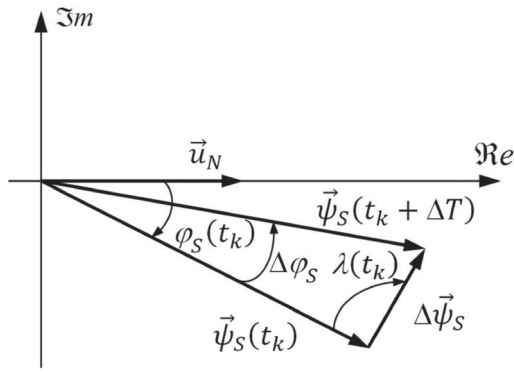


Figure 2. Stator flux vectors in the complex plane.

the beginning of the control period determined with respect to the centre of the sector, $\Delta\varphi_S$ is the stator flux vector argument change in the control period and $\lambda(t_k)$ is an angle of a triangle formed by the stator flux vectors. An analysis of the voltage vectors influence on the stator flux vector magnitude can be simplified with suppositions that the influence of cables which connect IM with the inverter, the inverter semiconductors voltage drops, the influence of the inverter dead time and the stator resistance voltage drop are neglected.

Then, the magnitude of vector $\Delta\vec{\psi}_S$ shown in Figure 2 is approximately:

$$|\Delta\vec{\psi}_S| \approx \begin{matrix} u_{dc}T \\ 0 \end{matrix} \begin{matrix} \vec{u}_j, j = 1, \dots, 6 \\ \vec{u}_0, \vec{u}_7 \end{matrix} \quad (10)$$

The angle $\lambda(t_k)$ shown in Figure 2, can be calculated from the known angle $\varphi_S(t_k)$ and from the position of the applied voltage vector in the complex plane.

The stator flux vector magnitude $|\vec{\psi}_S(t_k + \Delta T)|$ at the end of the control period and the stator flux vector argument change $\Delta\varphi_S$ in the control period can then be calculated using the law of cosines:

$$|\vec{\psi}_S(t_k + \Delta T)| \approx \sqrt{|\vec{\psi}_S(t_k)|^2 + |\Delta\vec{\psi}_S|^2 - 2|\vec{\psi}_S(t_k)||\Delta\vec{\psi}_S|\cos[\lambda(t_k)]} \quad (11)$$

$$\Delta\varphi_S \approx \cos^{-1} \left[\frac{|\vec{\psi}_S(t_k + \Delta T)|^2 + |\vec{\psi}_S(t_k)|^2 - |\Delta\vec{\psi}_S|^2}{2|\vec{\psi}_S(t_k + \Delta T)||\vec{\psi}_S(t_k)|} \right] \quad (12)$$

A change of the electromagnetic torque is:

$$\Delta t_{\text{elm}} = t_{\text{elm}}(t_k + T) - t_{\text{elm}}(t_k) \quad (13)$$

where Δt_{elm} is the change of the electromagnetic torque in the control period, $t_{\text{elm}}(t_k + \Delta T)$ is the electromagnetic torque at the end of the control period and $t_{\text{elm}}(t_k)$ is the electromagnetic torque at the beginning of the control period.

It can be assumed that the IM parameters are not changed during the control period and that the rotor

flux vector locus is practically a circle owing to the first order, low-pass filtering action between the stator and the rotor flux vectors. If another equation for the electromagnetic torque, which is equivalent to Equation (4), is used:

$$t_{\text{elm}} = \frac{3}{2} p \frac{L_m}{\sigma L_S L_R} |\vec{\psi}_S| |\vec{\psi}_R| \sin(\gamma) \quad (14)$$

the following is derived from Equations (2–4, 14):

$$\frac{t_{\text{elm}}(t_k + \Delta T)}{t_{\text{elm}}(t_k)} \approx \frac{|\vec{\psi}_S(t_k + T)| \sin[\gamma(t_k + \Delta T)]}{|\vec{\psi}_S(t_k)| \sin[\gamma(t_k)]} \quad (15)$$

$$\gamma(t_k) = \sin^{-1} \left\{ \frac{|\vec{i}_S(t_k) \sin[\delta(t_k)]|}{\left| \frac{1}{\sigma L_S} \vec{\psi}_S(t_k) - \vec{i}_S(t_k) \right|} \right\} \quad (16)$$

$$\gamma(t_k + \Delta T) = \gamma(t_k) + \Delta\gamma \quad (17)$$

$$\Delta\gamma = \Delta\varphi_S - \Delta\varphi_R \quad (18)$$

where γ is the angle between the stator flux and the rotor flux vectors, $\gamma(t_k + \Delta T)$ is the angle between the stator flux and the rotor flux vectors at the end of the control period and $\gamma(t_k)$ is the angle between the stator flux and the rotor flux vectors at the beginning of the control period.

$\Delta\varphi_S$ in Equation (18) is the stator flux vector argument change in the control period and can be calculated from Equation (12). In a stationary $\alpha\beta$ -reference frame both the stator flux and the rotor flux vectors rotate at an equal average angular speed. $\Delta\varphi_R$ is the rotor flux vector argument change in the control period and it can be calculated from the average angular speed of the stator flux vector and the control period:

$$\Delta\varphi_R \approx (d_S/dt)_{AV} \Delta T \quad (19)$$

where $(d\varphi_S/dt)_{AV}$ is the average angular speed of the stator flux vector.

Finally, the change of the electromagnetic torque Δt_{elm} in the control period can be calculated using Equations (9–19):

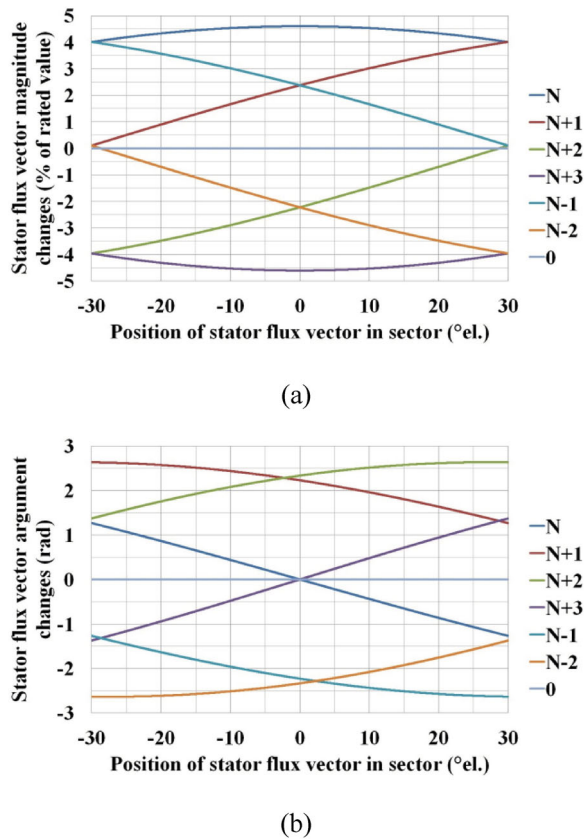
$$\Delta t_{\text{elm}} \approx t_{\text{elm}}(t_k) \frac{|\vec{\psi}_S(t_k)| + |\Delta\vec{\psi}_S|}{|\vec{\psi}_S(t_k)|} \times \{ \cos(\Delta\gamma) + ctg[\gamma(t_k)] \sin(\Delta\gamma) \} - t_{\text{elm}}(t_k) \quad (20)$$

The changes of the control variables are calculated from the stator variables and in comparison with the conventional DTC method, the only additionally required parameter is the IM total leakage inductance σL_S used in Equation (16).

The paper analyzes the main propulsion drive of the low-floor tram series TMK 2200 produced by Končar and operating in the city of Zagreb. The drive consists of

Table 1. Traction motor data.

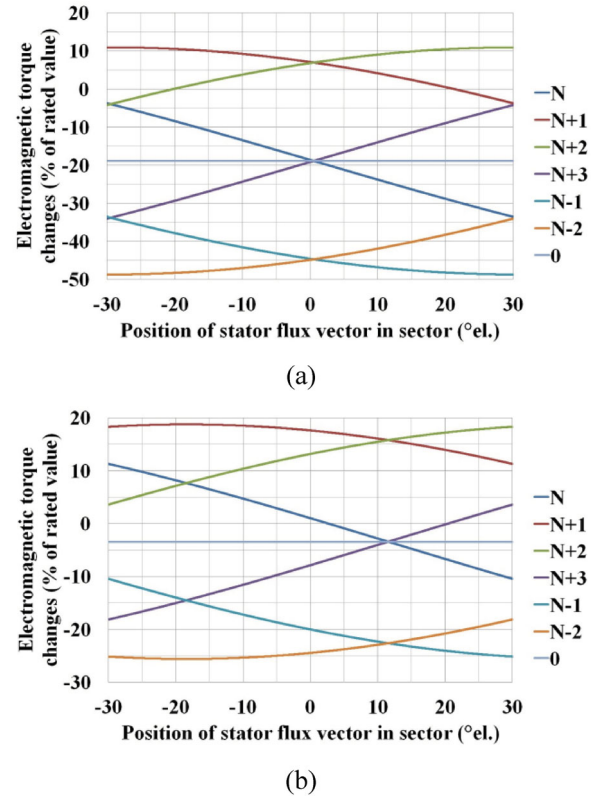
Rated power (kW)	65	Stator resistance (Ω)	0.044
Rated voltage (V)	320	Stator leakage inductance (mH)	0.263
Rated current (A)	151	Mutual inductance (mH)	8.9
Rated frequency (Hz)	58	Rotor resistance (Ω)	0.025
Number of pole pairs	2	Rotor leakage inductance (mH)	0.350
Rated speed (min^{-1})	1700		

**Figure 3.** Stator flux vector changes for all voltage vectors (d.c. link voltage 600 V, control period 80 μs , the reference value of the stator flux vector magnitude is equal to the rated value): (a) magnitude changes and (b) argument changes.

three inverters and each inverter supplies two traction motors connected in parallel. The data of the motor are given in Table 1, the rated value of the overhead catenary voltage in Zagreb is 600 V and the control period is 80 μs .

Figure 3 shows the stator flux vector magnitude (a) and argument changes (b) with respect to the stator flux vector position in the sector for all voltage vectors. The reference value of the stator flux vector magnitude is equal to the rated value, the value of the d.c. link voltage u_{dc} is 600 V and the control period ΔT is 80 μs . The changes of the stator flux vector magnitude are shown relatively to the rated value and the analysis is simplified with the supposition that $|\vec{\psi}_S(t_k)|$ used in Equations (11–12) is equal to the reference value. Although the changes in the stator flux vector magnitude are derived in a different way, the results coincide closely with the results presented in [32–36].

Figure 4(a) shows changes of the electromagnetic torque Δt_{elm} at the rated speed n_n and with an average

**Figure 4.** Electromagnetic torque changes for all voltage vectors (d.c. link voltage 600 V, control period 80 μs): (a) rated speed, 25% rated torque and (b) 25% rated speed, rated torque.

value of the torque equal to 25% of the rated torque T_n and Figure 4(b) shows changes of the electromagnetic torque Δt_{elm} at 25% of the rated speed and with an average value of the torque equal to the rated torque. The reference value of the stator flux vector magnitude is equal to the rated value, the value of the d.c. link voltage is 600 V and the control period is 80 μs . The electromagnetic torque changes are shown relatively to the rated torque. For the purpose of ease of analysis, Δt_{elm} is calculated from Equation (20) with the value of the electromagnetic torque at the beginning of the control period $t_{elm}(t_k)$ equal to the average value of the torque and with the value of the angle between the stator flux and the rotor flux vectors at the beginning of the control period $\gamma(t_k)$ in Equation (16) equal to the average value. The torque changes shown in Figure 4(a) are typical of higher speeds and those shown in Figure 4(b) are typical of lower speeds. The obtained results coincide closely with the results presented in [33,36].

From Figures 3 and 4 it can be concluded that the influence of each voltage vector on control variables depends not only on the speed and load but also on the actual position of the stator flux vector in the sector.

2.4. MPTC algorithm

Since the direct torque control is considered here, the most interesting task is to reduce the torque ripple. The basis of the MPTC algorithm is derived according to

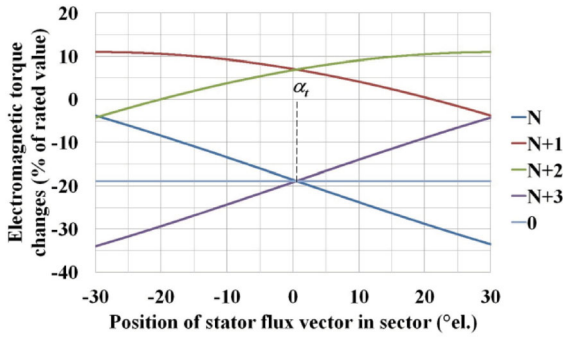


Figure 5. Electromagnetic torque changes (d.c. link voltage 600 V, control period 80 μ s, rated speed, 25% rated torque).

the control variables changes shown in Figures 3 and 4. The electromagnetic torque changes shown in Figure 4 represent potential change of the torque in the control period and can be used for the torque ripple reduction if future values of the torque are predicted. If the horizon one predictive control is applied, the voltage vector which would cause minimum deviation of the torque from the reference value at the end of the next control period should be used. The above mentioned consideration means that an absolute value of the torque changes should be as small as possible but the influence of the voltage vector on the stator flux vector magnitude should be taken into account. In Figure 4 it can be seen that an absolute value of the torque changes for reverse active voltage vectors \vec{u}_{N-1} and \vec{u}_{N-2} are greater than the torque changes for other voltage vectors and these vectors should not be used for counter clockwise movement direction. The torque changes shown in Figure 4 are again shown in Figure 5 but without the results for voltage vectors \vec{u}_{N-1} and \vec{u}_{N-2} . It should be noted that for the given speed and load there is an angle in the sector at which the changes in the torque of voltage vectors \vec{u}_N , \vec{u}_{N+3} and \vec{u}_0 are equal (this angle is in Figure 5 denoted by α_t). With regard to the torque, voltage vectors \vec{u}_N , \vec{u}_{N+1} , \vec{u}_{N+2} and \vec{u}_0 should be considered for the stator flux vector angles less than the angle α_t , and for the stator flux vector angles greater than the angle α_t , voltage vectors \vec{u}_{N+1} , \vec{u}_{N+2} , \vec{u}_{N+3} and \vec{u}_0 should be considered.

The predicted position of the stator flux vector in the sector at the beginning of the next control period $\varphi_S^P(k+1)$ is calculated from Equation (7) and is compared with the angle α_t . In order to take the influence of the voltage vector on the stator flux vector magnitude into account, the estimated stator flux vector magnitude calculated from Equation (8) is compared with the reference value ψ_{Sref} and four different cases can be distinguished. For each case, three different voltage vectors should be taken into consideration:

$$\begin{aligned} 1^\circ \varphi_S^P(k+1) \leq \alpha_t, |\vec{\psi}_S^P(k+1)| \leq \psi_{Sref} \\ \Rightarrow \vec{u}_{P1} = \vec{u}_N, \vec{u}_{P2} = \vec{u}_{N+1}, \vec{u}_{P3} = \vec{u}_0 \end{aligned} \quad (21a)$$

$$\begin{aligned} 2^\circ \varphi_S^P(k+1) \leq \alpha_t, |\vec{\psi}_S^P(k+1)| > \psi_{Sref} \\ \Rightarrow \vec{u}_{P1} = \vec{u}_{N+1}, \vec{u}_{P2} = \vec{u}_{N+2}, \vec{u}_{P3} = \vec{u}_0 \end{aligned} \quad (21b)$$

$$\begin{aligned} 3^\circ \varphi_S^P(k+1) > \alpha_t, |\vec{\psi}_S^P(k+1)| \leq \psi_{Sref} \\ \Rightarrow \vec{u}_{P1} = \vec{u}_{N+1}, \vec{u}_{P2} = \vec{u}_{N+2}, \vec{u}_{P3} = \vec{u}_0 \end{aligned} \quad (21c)$$

$$\begin{aligned} 4^\circ \varphi_S^P(k+1) > \alpha_t, |\vec{\psi}_S^P(k+1)| > \psi_{Sref} \\ \Rightarrow \vec{u}_{P1} = \vec{u}_{N+2}, \vec{u}_{P2} = \vec{u}_{N+3}, \vec{u}_{P3} = \vec{u}_0 \end{aligned} \quad (21d)$$

where \vec{u}_{Pj} are voltage vectors that are used for the torque prediction and could be potentially applied in the next control period and.

The voltage vectors defined in the first and the fourth case would correctly influence the stator flux vector magnitude. In the second case, voltage vector \vec{u}_{N+1} would increase the stator flux vector magnitude and would not satisfy the demand for a stator flux vector magnitude decrease, but it is taken into consideration due to the fact that at some operating points this voltage vector is the only voltage vector which increases the torque at the beginning of the sector, as can be seen in Figure 4(a). Similarly, in the third case, voltage vector \vec{u}_{N+2} is taken into consideration because at some operating conditions it is the only voltage vector which increases the torque at the end of the sector (Figure 4(a)).

The voltage vector which will be applied in the next control period is determined according to the predicted values of the torque (values at the beginning of the $(k+2)^{nd}$ control period) using equations derived in the previous chapter. Instead of the values at time instant $t = t_k$, the values at the beginning of the next, $(k+1)^{st}$ control period should be used, and the values at time instant $t = t_k + \Delta T$ correspond to the predicted values at the beginning of the $(k+2)^{nd}$ control period.

Then, in the MPTC is defined cost function which has to be minimized as follows:

$$g_j = |T_{ref} - t_{elm}^P(k+2)_j| \quad (22)$$

where g_j is the cost function and $t_{elm}^P(k+2)_j$ is the predicted value of the electromagnetic torque at the beginning of the $(k+2)^{nd}$ control period, subscript j indicates that the values of the predicted torque should be calculated for three different voltage vectors according to Equation (21) and T_{ref} is torque reference value.

The cost function from Equation (22) consists only of the difference between the reference and the predictive value of the torque and the use of the weighting factors is avoided, which is a considerable advantage of the MPTC method in comparison with the PTC method. The influence of the voltage vectors on the stator flux vector magnitude is indirectly taken into account by defining different cases in Equation (21). The exception

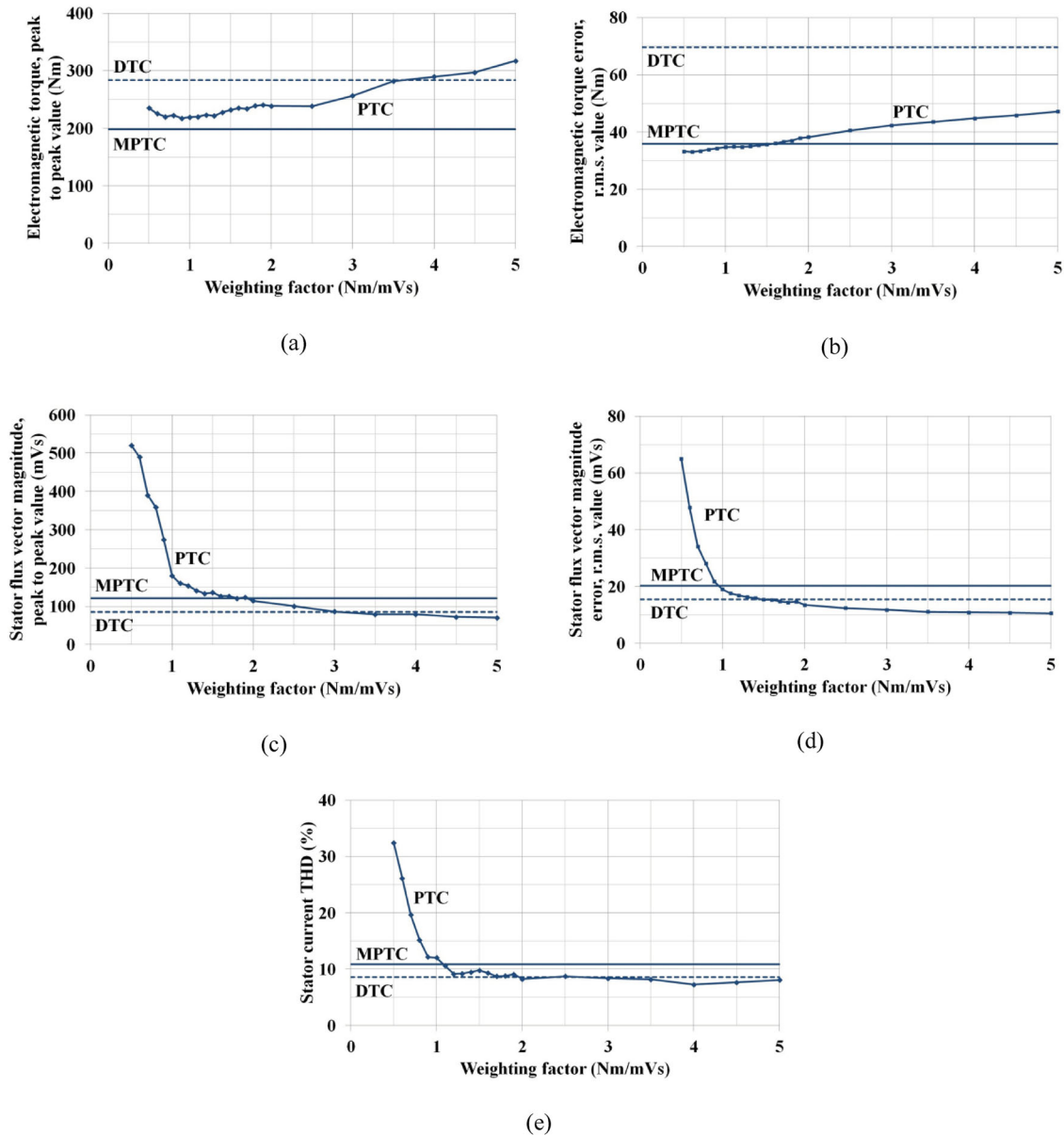


Figure 6. Simulation results, steady state (rated speed, rated torque, d.c. link voltage 600 V, control period 80 μ s): (a) electromagnetic torque, peak to peak value, (b) electromagnetic torque, r.m.s. value, (c) stator flux vector magnitude, peak to peak value, (d) stator flux vector magnitude, r.m.s. value and (e) stator current THD.

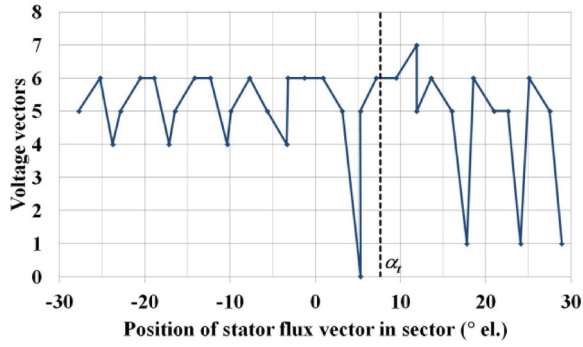
is a potential use of \vec{u}_{N+1} when the stator flux vector magnitude should be decreased, Equation (21b), and a potential use of \vec{u}_{N+2} when the stator flux vector magnitude should be increased, Equation (21c). These voltage vectors are used only if the predicted values of the stator flux vector magnitude are within hysteresis bounds (similar to the conventional DTC method). Otherwise, the cost function should be minimized for other two voltage vectors.

The only operating points at which the reverse active vectors should be used for counter clockwise direction of rotation are low speeds and negative torque reference. However, these operating points can be detected and the control algorithm defined with Equation (21) should be slightly modified, and again, the predicted values for only three voltage vectors should be calculated. For the clockwise direction of rotation, voltage

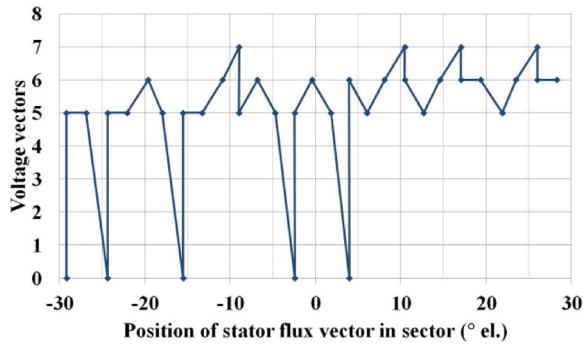
vector \vec{u}_{N-1} should be used instead of \vec{u}_{N+1} and voltage vector \vec{u}_{N-2} should be used instead of \vec{u}_{N+2} .

3. Simulation results

The performances of the MPTC method, the conventional DTC method, and the PTC method are compared with the simulation results at steady states. The simulations were carried out with the value of the control period of 80 μ s and with constant IM parameters. In the conventional DTC method the hysteresis bands of both the torque and the flux comparators are purposely set to zero in order to achieve the smallest torque and stator flux ripple. For the calculation of the predicted stator current vector $\vec{i}_s^p(k+1)$, Equation (6), the control period ΔT is divided into five equal time instants and the measurements of the stator currents take place

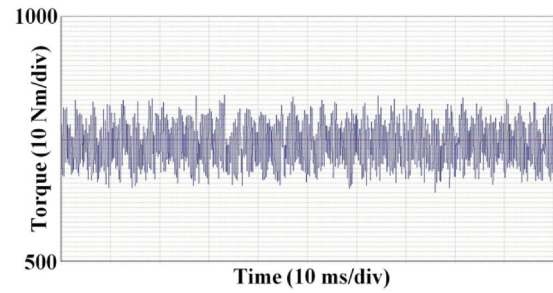


(a)

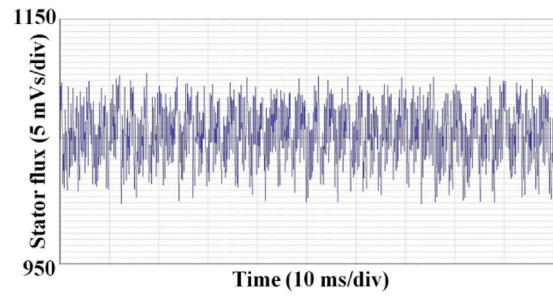


(b)

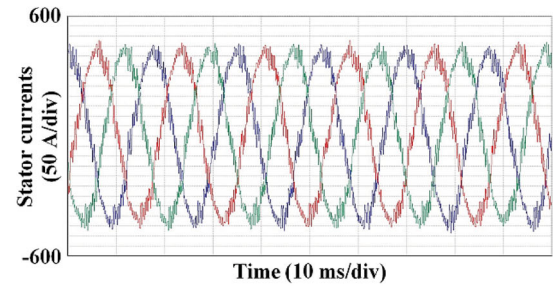
Figure 7. Simulation results, PTC method, steady state (rated speed, rated torque, sector 4, d.c. link voltage 600 V, control period 80 μ s): (a) weighting factor 1 Nm/mVs and (b) weighting factor 4 Nm/mVs.



(a)



(b)

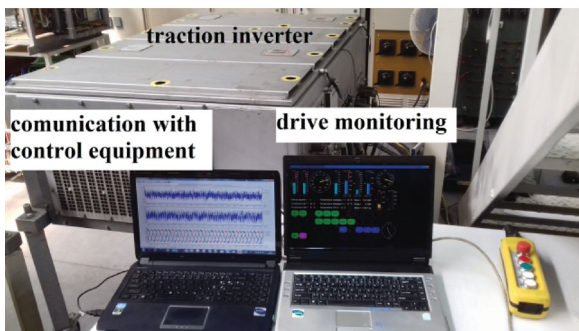


(c)

Figure 9. Experimental results, MPTC method, steady state (rated speed, rated torque, control period 80 μ s): (a) estimated torque, (b) estimated stator flux vector magnitude, (c) measured stator currents.



(a)



(b)

Figure 8. Experimental setup: (a) d.c. load machine and traction motors and (b) traction inverter, communication with control equipment and drive monitoring.

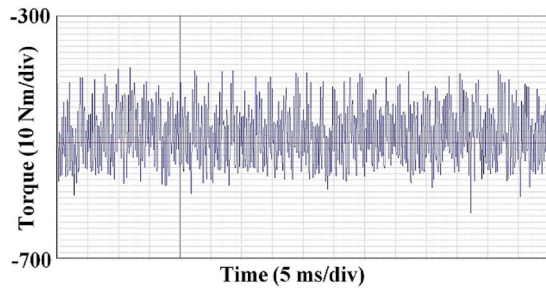
at the beginning of the control period, after 16 μ s, and after 32 μ s. In order to quantify the comparison of the methods, peak to peak values of the control variables, r.m.s. values of the control variables errors defined with the difference between the actual and the reference values and the stator current THD are determined.

In the PTC method, the cost function requires the weighting factor of the stator flux vector magnitude:

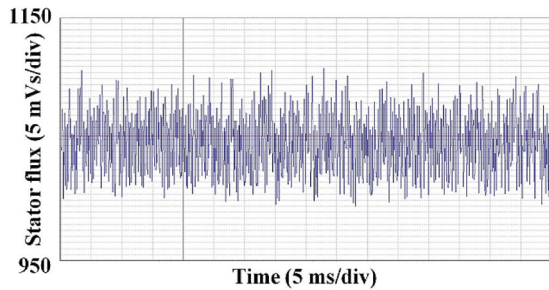
$$g_j = |T_{ref} - t_{elm}^P(k+2)| + \lambda_\psi |\psi_{Sref} - |\vec{\psi}_S^P(k+2)||, \quad j = 0, \dots, 7 \quad (23)$$

where λ_ψ is the weighting factor which allows adjusting the importance of the flux error with respect to the torque error.

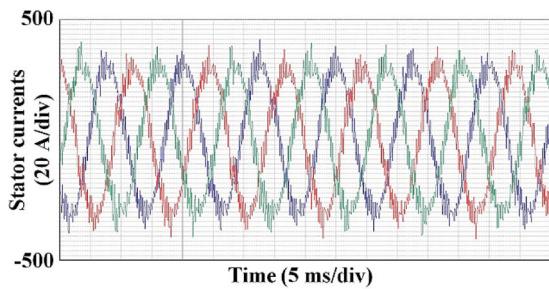
Figure 6 shows simulation results of the PTC method for different values of the weighting factor (the results obtained in the conventional DTC method and the MPTC method are also presented), at the rated speed



(a)



(b)



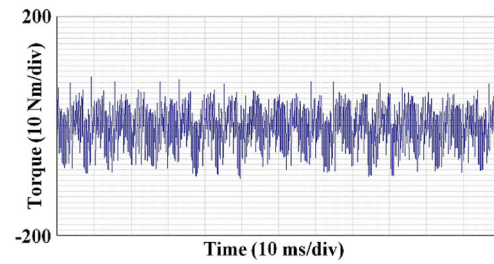
(c)

Figure 10. Experimental results, MPTC method, steady state (150% rated speed, -66.7% rated torque, control period $80 \mu\text{s}$): (a) estimated torque, (b) estimated stator flux vector magnitude, (c) measured stator currents.

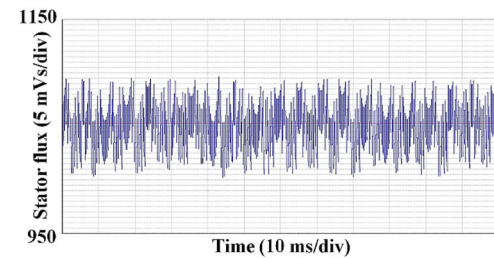
and with an average value of the torque equal to the rated torque.

It can be concluded from Figure 6 that the MPTC method is superior regarding the torque peak to peak value, and the torque error r.m.s. value in the MPTC method is very close to the minimum value obtained in the PTC method. It should be pointed out that in the PTC method the torque error r.m.s. minimum value is achieved with the weighting factor which results in the large stator flux vector magnitude ripple and, consequently, the large stator current THD.

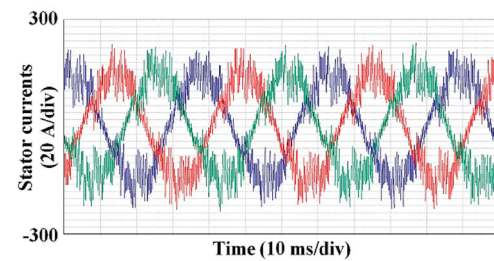
Some suppositions made in the MPTC methods are indirectly confirmed when the PTC method is applied. Figure 7 shows the control signals for inverter semi-conductors at the rated speed and the average value of the electromagnetic torque equal to the rated value for two different values of the weighting factor λ_{ψ} . It can be seen that for a smaller value of the weighting factor, when the actual position of the stator flux vector



(a)

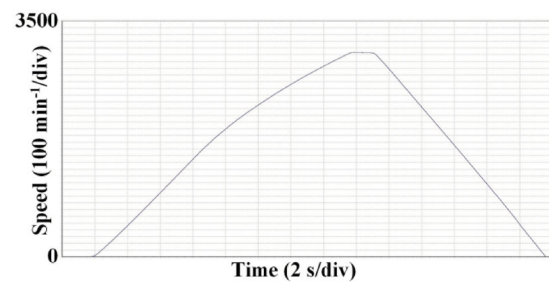


(b)

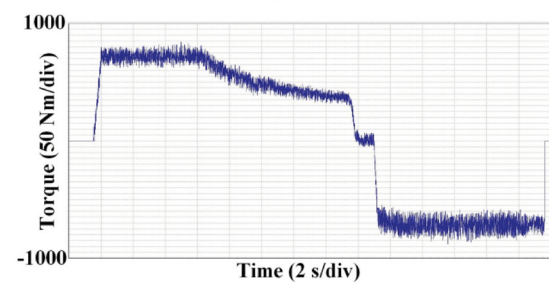


(c)

Figure 11. Experimental results, MPTC method, steady state (50% rated speed, zero average torque value, control period $80 \mu\text{s}$): (a) estimated torque, (b) estimated stator flux vector magnitude, (c) measured stator currents.



(a)



(b)

Figure 12. Experimental results, MPTC method, acceleration and deceleration of the drive: (a) motor speed, (b) estimated torque.

in the sector is smaller than the angle α_t , voltage vectors $\vec{u}_N, \vec{u}_{N+1}, \vec{u}_{N+2}$ and \vec{u}_0 or \vec{u}_7 are applied and when the actual position of the stator flux vector in the sector is greater than α_t , instead of voltage vector \vec{u}_N, \vec{u}_{N+3} is applied. For a larger value of the weighting factor, the PTC method uses the same voltage vectors as in the conventional DTC method, i.e. $\vec{u}_{N+1}, \vec{u}_{N+2}$ and \vec{u}_0 or \vec{u}_7 .

4. Experimental results

Experiments were carried out on a model of the main propulsion drive of the low-floor tram series TMK 2200

operating in the city of Zagreb and produced by Končar. The model consists of an inverter which supplies two traction motors and both motors are mechanically coupled to a 600 kW d.c. load machine. The experimental setup is shown in Figure 8. Control algorithms were programmed in the floating-point digital signal processor TMS320F28335. The control period was 80 μ s and the measurements of the stator currents were carried out at the beginning of the control period, after 16 μ s, and after 32 μ s.

Figure 9 shows experimental steady-state results of the MPTC method at the rated speed and with an average value of the estimated torque equal to the rated

Table 2. Experimental results.

n/n_n	t_{elm}/T_n	Method	Torque, peak to peak value (Nm)	Torque error, r.m.s. value (Nm)	Stator flux magnitude, peak to peak value (mVs)	Stator flux magnitude error, r.m.s. value (mVs)	Stator current THD (%)
0.5	1	DTC	284.2	49.6	88.1	17.9	10.8
		MPTC	240.0	34.6	104.2	21.1	11.0
		PTC, Vs 1.5 Nm/m	269.5	38.6	111.7	15.4	9.0
		PTC, 4 Nm/mVs	319.0	51.5	62.7	10.6	8.2
	0	DTC	245.7	49.3	79.8	18.8	27.9
		MPTC	183.8	30.3	104.3	22.4	30.0
		PTC, 1.5 Nm/mVs	209.6	34.0	114.7	16.0	23.1
		PTC, 4 Nm/mVs	299.0	46.7	66.8	11.3	21.7
	-1	DTC	350.6	129.6	113.0	27.8	14.8
		MPTC	280.5	55.2	135.5	32.7	16.3
		PTC, 1.5 Nm/mVs	288.6	58.4	131.3	24.2	13.1
		PTC, 4 Nm/mVs	369.2	78.6	86.0	16.8	13.4
1	1	DTC	367.4	77.9	87.9	17.4	11.0
		MPTC	252.7	40.5	111.1	21.9	11.6
		PTC, 1.5 Nm/mVs	247.5	43.2	129.8	15.9	9.6
		PTC, 4 Nm/mVs	303.0	53.4	68.7	11.5	8.6
	0	DTC	278.2	55.4	88.8	17.2	27.3
		MPTC	203.5	32.4	108.5	19.9	27.6
		PTC, 1.5 Nm/mVs	219.2	33.6	127.9	16.3	23.6
		PTC, 4 Nm/mVs	292.6	43.6	66.2	11.1	20.2
	-1	DTC	346.9	65.7	105.7	22.6	15.0
		MPTC	295.4	44.8	134.9	28.0	14.9
		PTC, 1.5 Nm/mVs	329.4	49.8	150.9	19.8	12.9
		PTC, 4 Nm/mVs	462.4	67.4	84.7	13.8	12.8
1.5	1	DTC	304.2	98.8	88.7	17.0	14.2
		MPTC	193.6	37.0	108.7	21.9	15.2
		PTC, 1.5 Nm/mVs	216.5	40.8	101.8	15.7	12.0
		PTC, 4 Nm/mVs	254.6	50.7	66.8	11.8	11.3
	0	DTC	222.3	76.5	86.8	16.3	35.3
		MPTC	182.7	30.1	108.2	22.5	39.4
		PTC, Vs 1.5 Nm/m	183.2	34.8	104.2	15.5	30.4
		PTC, 4 Nm/mVs	222.0	38.2	64.9	12.3	28.4
	-1	DTC	369.6	81.9	108.3	21.5	17.5
		MPTC	257.6	44.7	129.7	23.8	17.6
		PTC, 1.5 Nm/mVs	273.1	45.7	156.7	20.8	15.9
		PTC, 4 Nm/mVs	327.4	58.5	86.8	13.2	14.3

torque, Figure 10 shows results at 150% of the rated speed and with an average value of the torque equal to -66.7% of the rated torque and Figure 11 shows results at 50% of the rated speed and with an average value of the torque equal zero.

The dynamic performance of the MPTC method is confirmed by the acceleration and the deceleration of the drive (traction and braking mode of the drive), which is shown in Figure 12.

The MPTC method is compared with the conventional DTC method and with the PTC method (two weighting factors are used). In order to fairly compare the MPTC method with the PTC method, the predicted values of the control variables used in the cost function when the PTC method is applied, Equation (23), are calculated in the same way as when the MPTC method is applied as described in chapter 2.4., i.e. a potential mismatch between the real IM parameters and speed and the parameters and speed used for the prediction is avoided. Due to a higher computational burden, the algorithm used in the PTC method could not be executed in $80\ \mu\text{s}$ and therefore was increased to $90\ \mu\text{s}$. The steady state results for the control period of $90\ \mu\text{s}$ for all methods are summarized in Table 2.

From Table 2 it can be concluded that the MPTC method is superior to other two methods regarding torque ripple. The stator flux magnitude ripple as well as the stator current THD is in the case of the MPTC method slightly increased compared with the conventional DTC method. Although the steady state performance of the drive could be improved with the application of the PTC method with different values of the weighting factor, it should be pointed out that for each operating point too low values of the weighting factor of the stator flux vector magnitude would produce high oscillations in the stator flux and in the stator currents, and if the values of the weighting factor are too high, the control of the electromagnetic torque might be lost.

5. Conclusion

This paper proposes an MPTC method which can be applied for high performance IM drives. The MPTC method and the conventional DTC method use an IM dynamic model with the stator variables only and the required IM parameter for the estimation of the control variables is the stator resistance. On the other hand, the PTC method estimates both the stator and the rotor variables and uses all IM parameters and the speed. The MPTC method and the conventional DTC method have some steady state and dynamic performances, but the control of the torque and the stator flux vector magnitude is preserved regardless of the operating point and the performance of the PTC method might be significantly adversely affected if an improper weighting factor is used. Another disadvantage of the

PTC method is high computational burden due to the required prediction of control variables for all possible voltage vectors (seven voltage vectors for a two-level three-phase VSI). When the MPTC method is applied, the predicted values of three voltage vectors should be calculated.

The simulation and experimental results show that in the case of the MPTC method torque ripple are reduced compared with the conventional DTC method and are similar when the PTC method with smaller values of the weighting factor is applied. This fact as well as insensitivity of the MPTC method to the IM parameter variation, except to the stator resistance and the IM total leakage inductance, makes the MPTC method very robust and suitable for e.g. traction drives.

Disclosure statement

No potential conflict of interest was reported by the authors.

ORCID

Damir Sumina  <http://orcid.org/0000-0001-8474-125X>

References

- [1] Nash JN. Direct torque control, induction motor vector control without an encoder. *IEEE Trans Industry Appl.* 1997;33(2):333–341.
- [2] Casadei D, Profumo F, Serra G. FOC and DTC: two viable schemes for induction motors torque control. *IEEE Trans Power Electron.* 2002;17(5):779–787.
- [3] Depenbrock M. Direkte Selbstregelung (DSR) für hochdynamische Drehfeldantriebe mit Stromrichter-speisung. *etzArchiv.* 1985;7:211–218.
- [4] Depenbrock M. Direct self-control (DSC) of inverter-fed induction machine. *IEEE Trans Power Electron.* 1988;3(4):420–429.
- [5] Takahashi I, Noguchi T. A new quick-response and high-efficiency control strategy of an induction motor. *IEEE Trans Industry Appl.* 1986;IA-22(5):820–827.
- [6] Tiitinen P, Pohjalainen P, Lalu J. The next generation motor control method: direct torque control (DTC). *Eur Power Electr Drives J.* 1995;5(1):14–18.
- [7] Buja GS, Kazmierkowski MP. Direct torque control of PWM inverter-fed AC motors—A survey. *IEEE Trans Ind Electron.* 2004;51(4):744–757.
- [8] Telford D, Dunnigan MW, Williams BW. A comparison of vector control and direct torque control of an induction machine. 2000 Proceedings of the 31st IEEE Annual Power Electronics Specialists Conference; 2000 June 18–23; Galway, Ireland; 2000. p. 421–426.
- [9] Krušelj D. Methods for direct torque control of induction machines. 2017 Proceedings of the 19th International Conference on Electrical Drives and Power Electronics; 2017 Oct 4–6; Dubrovnik, Croatia; 2017.
- [10] Sutikno T, Idris NRN. A review of direct torque control of induction motors for sustainable reliability and energy efficient drives. *ELSEVIER Renew Sustain Energy Rev.* 2014;32:548–558.
- [11] Kumar RH, Iqbal A, Lenin NC. Review of recent advancements of direct torque control in induction motor drives – a decade of progress. *IET Power Electr.* 2018;11(1):1–15.

- [12] Cortés P, Kazmierkowski MP, Kennel RM, et al. Predictive control in power electronics and drives. *IEEE Trans Ind Electron.* 2008;55(12):4312–4324.
- [13] Kuoro S, Cortés P, Vargas R, et al. Model predictive control—a simple and powerful method to control power converters. *IEEE Trans Ind Electron.* 2009;56(6):1826–1838.
- [14] Bariša T, Ileš Š, Sumina D, et al. Model predictive direct current control of a permanent magnet synchronous generator based on Flexible Lyapunov function considering converter dead time. *IEEE Trans Industry Appl.* 2018;54(3):2899–2912.
- [15] Kuoro S, Perez MA, Rodríguez J, Llor AM, Young HA. Model predictive control: MPC's Role in the Evolution of power electronics. *IEEE Ind Electron Mag.* 2015;9(Dec):8–21.
- [16] Vazquez S, Rodríguez J, Rivera M, et al. Model predictive control for power converters and drives: advances and Trends. *IEEE Trans Ind Electron.* 2017;64(2):935–947.
- [17] Miranda H, Cortés P, Yuz JI, et al. Predictive torque control of induction machines based on state-space Models. *IEEE Trans Ind Electron.* 2009;56(6):1916–1924.
- [18] Wang F, Li S, Mei X, et al. Model-based predictive direct control strategies for electrical drives: an experimental evaluation of PTC and PCC methods. *IEEE Trans Ind Inform.* 2015;11(3):671–681.
- [19] Zhang Y, Xia B, Yang H, et al. Overview of model predictive control for induction motor drives. *Chinese J Electr Eng.* 2016;2(1):62–76.
- [20] Wang F, Mei X, Rodríguez J, et al. Model predictive control for electrical drive systems – an overview. *CES Trans Electr Mach Syst.* 2017;1(3):219–230.
- [21] Wang F, Davari SA, Chen Z, et al. Finite control set model predictive control of induction machine with a robust adaptive observer. *IEEE Trans Ind Electron.* 2017;64(4):2631–2641.
- [22] Ouhrouche M, Errouissi R, Trzynadlowski AM, et al. A novel predictive direct torque controller for induction motor drives. *IEEE Trans Ind Electron.* 2016;63(8):5221–5230.
- [23] Zhang Y, Yang H. Two-vector-based model predictive torque control without weighting factors for induction motor drives. *IEEE Trans Power Electron.* 2016;31(2):381–1390.
- [24] Nikzad MR, Asaei B, Ahmadi SO. Discrete duty-cycle-control method for direct torque control of induction motor drives with model predictive solution. *IEEE Trans Power Electron.* 2018;33(3):2317–2329.
- [25] Davari SA, Khaburi DA, Kennel R. An improved FCS-MPC algorithm for an induction motor with an imposed optimized weighting factor. *IEEE Trans Power Electron.* 2012;27(3):1540–1551.
- [26] Amiri M, Milimonfared J, Khaburi DA. Predictive torque control implementation for induction motors based on discrete space vector modulation. *IEEE Trans Ind Electron.* 2018;65(9):6881–6889.
- [27] Habibullah M, Lu DDC, Xiao D, et al. A simplified finite-state predictive direct torque control for induction motor drive. *IEEE Trans Ind Electron.* 2016;63(6):3964–3975.
- [28] Cortés P, Kuoro S, La Rocca B, Vargas R, Rodríguez J, Leon JI, Vazquez S, Franquelo LG. Guidelines for weighting factors adjustment in finite state model predictive control of power converters and drives. 2009 Proceedings of the IEEE Conference Industrial Technology; 2009 Feb 10–13; Gippsland, Australia; 2009. p. 1–7.
- [29] Rojas CA, Rodríguez J, Villarroel F, et al. Predictive torque and flux control without weighting factors. *IEEE Trans Ind Electron.* 2013;60(2):681–690.
- [30] Davari SA, Rodríguez J. Predictive direct voltage control of induction motor with mechanical model consideration for sensorless applications. *IEEE J Emerg Sel Top Power Electr.* 2018;64(4):2631–2641.
- [31] Kaboli S, Zolghadri MR, Eskandri P, et al. Prediction algorithm for torque ripple reduction in DTC-based drives. *Iran J Sci Technol Trans A.* 2008;31(4):343–355.
- [32] Chen J, Li Y. Virtual vectors based predictive control of torque and flux of induction motor and speed sensorless drives. 1999 Proceedings of the 34th IEEE Industry Applications Society Conference; 1999 Oct 3–7; Phoenix, USA; 1999. p. 2606–2613.
- [33] Ambrožič V, Buja GS, Menis R. Band-constrained technique for direct torque control of induction motor. *IEEE Trans Ind Electron.* 2004;51(4):776–784.
- [34] Ambrožič V, Bertoluzzo M, Buja GS, et al. An assessment of the inverter switching characteristics in DTC induction motor drives. *IEEE Trans Power Electron.* 2005;20(2):457–465.
- [35] Zhang Y, Wang Q, Liu W. Direct torque control Strategy of induction motors based on predictive control and Synthetic vector duty Ratio control. 2010 Proceedings of the International Conference on Artificial Intelligence and Computational Intelligence; 2010 Oct 23–24; Sanya, China; 2010. p. 96–101.
- [36] Krušelj D. Novel prediction Technique for direct torque control of induction motor. 2014 Proceedings of the 21st International Conference on Electrical Machines; 2014 Sep 2–5; Berlin, Germany; 2014. p. 829–835.